16th East Asia-Pacific Conference on Structural Engineering & Construction (EASEC16)
Brisbane, Australia, December 3-6, 2019

STRUCTURAL BEHAVIOUR OF HIGH STRENGTH S690 COLD-FORMED STRUCTURAL HOLLOW SECTIONS UNDER COMPRESSION

M. XIAO[1,2] and K. F. CHUNG[1,2,*]

[1] Chinese National Engineering Research Centre for Steel Construction (Hong Kong Branch),
The Hong Kong Polytechnic University, Hong Kong SAR.
[2] Department of Civil and Environmental Engineering,
The Hong Kong Polytechnic University, Hong Kong SAR.
Emails: meng.ce.xiao@connect.polyu.hk, kwok-fai.chung@polyu.edu.hk
*Corresponding author

Abstract. *High strength steels are considered as efficient constructional materials due to their high strength-to-self-weight ratios. Over the past years, a large number of investigations into structural members made of high strength steels have proved that they meet various design requirements in both strength and ductility under various actions. However, the fabrication processes of these high strength steel sections are quite different from those made of normal strength steels, in particular, the presence of residual stresses due to both cold-forming and welding. In the current study, a total of eight cold-formed structural hollow sections (CFSHS) with different dimensions and fabrication methods are tested. The structural performance of these sections is examined with a total of 8 stocky column tests and 16 slender column tests. After comparing these measured resistances with the predicted resistances according to EN 1993-1-1, further works on improvements to the design method are suggested.*

Keywords: *High strength steels; Cold-formed sections; Classification of cross-sections; Section resistances; Member resistances.*

1. INTRODUCTION

High strength steels are considered as efficient constructional materials due to their high strength-to-self-weight ratios. With this remarkable advantage, low costs and energy consumption during production per unit weight have become the other two main advantages of high strength steels. Over the past years, a large number of investigations into structural members made of high strength steels have proved that they meet various design requirements in both strength and ductility under various actions (Ma et. al. 2017, Somodi and Kövesdi 2017). However, their fabrication processes are quite different from those members made of normal strength steels, in particular, the presence of residual stresses due to both cold-forming and welding are generally considered to affect adversely the structural performance of these cold-formed sections. Recently, the experimental studies into residual stresses of high strength steels have been carried out by several researchers, and the most commonly used methods to obtain residual stresses are the hole-drilling method and the sectioning method. Many researchers have compared measurements of the residual stresses among sections of different steel grades (Yang et. al. 2018). Numerical simulation is another effective method to study residual stresses. The coupled thermomechanical welding analysis has been developed with a calibrated heat source model (Godak et. al. 1984), and it enables accurate predictions on residual stress patterns for different sections with minimum laboratory work (Liu and Chung 2018, Wang 2018, Hu 2019). The residual stresses in the S690 welded H-sections obtained by finite element models or physical measurements may be directly incorporated into structural analyses, and buckling behaviour of both stocky and slender columns is subsequently simulated. These studies incorporating realistic residual stresses into column buckling are recently employed in high strength steel columns. It is found that these residual stresses have little effects on stocky columns of S690 welded H-sections, but they play an important role in slender columns of the same sections (Wang et. al. 2014, Li et. al. 2016). In the current study, a total of eight S690 cold-formed structural hollow sections (CFSHS) with different dimensions and fabrication methods are designed, and the structural performance of these sections are examined by with a total of 8 stocky column tests and 16 slender column tests.

2. FABRICATION AND MATERIAL PROPERTIES

2.1. Fabrication and Residual Stresses

A total of eight cold-formed structural hollow sections (CFSHS) are investigated in this study, and they are categorized into two series, i.e. Series SA and Series SB, as shown in Figure 1. These two series of sections are identical in their overall cross-sectional dimensions, but they are fabricated in different ways. For those sections of Series SA, two welds are made onto a pair of identical cold-bent C-shaped channels. For those sections of Series SB, a U-shaped channel is cold-bent, and welded onto a flat plate at both edges. The key differences between these two series of sections lie in two aspects: (1) Series SA sections are biaxially symmetric while Series SB sections are uniaxially symmetric; (2) Series SA sections have four cold-bent corners and two butt-welded side joints while Series SB sections have only two cold-bent corners and two butt-welded corner joints.

The residual stresses due to welding are predicted by using the coupled thermomechanical welding analysis, and the calibrated heat source model (Godak et. al. 1984) is adopted to simulate movement of the welding arch during welding. The simplified longitudinal residual stress patterns for these two series of sections are shown in Figure 2.

2.2. Material Properties

In the current study, 6 and 10 mm thick S690 plates are used to fabricate these CFSHS, and the results of standard coupon tests on these steel plates are presented in Table 1. The measured mechanical properties of the steel plates are compared with the requirements of EN 1993-1-12 (BSI 2007), and it should be noted that all these requirements are satisfied.

Table 1. Test results of standard coupon tests on S690 steel plates

Steel plate	f_y (N/mm^2)	f_u (N/mm^2)	Elongation limit (%)	$\frac{f_u}{f_y}$
6mm	733	807	16.2	1.09
10mm	754	813	17.7	1.06
EN 1993-1-12 (lower limit)	690	--	10.0	1.05

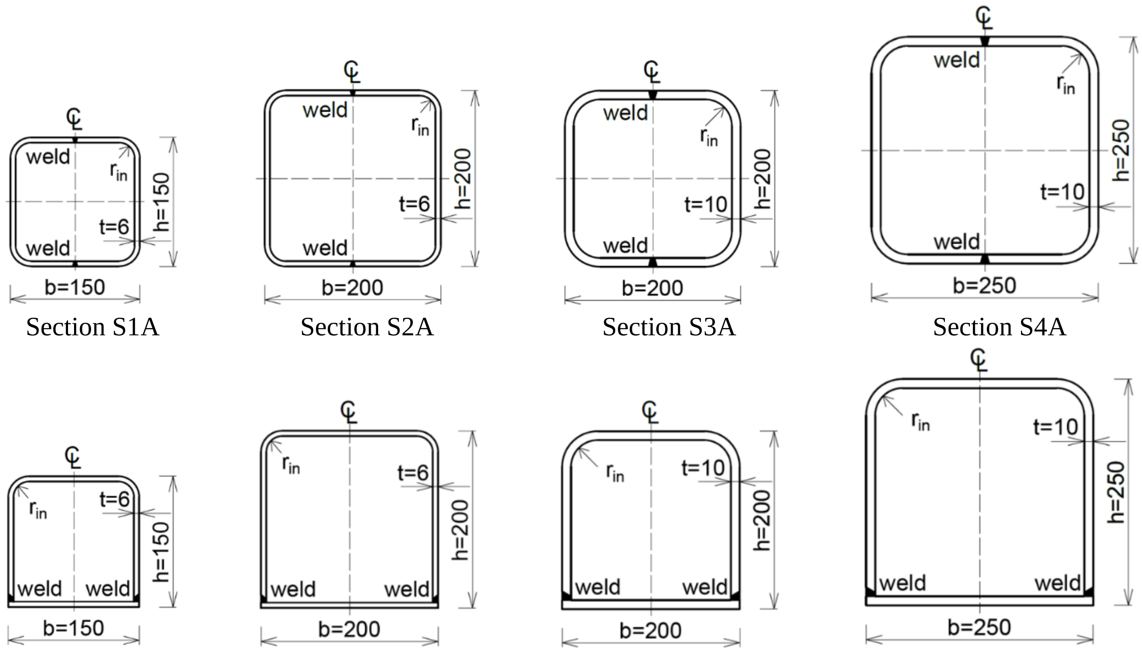

Figure 1. Dimensions of CFSHS sections

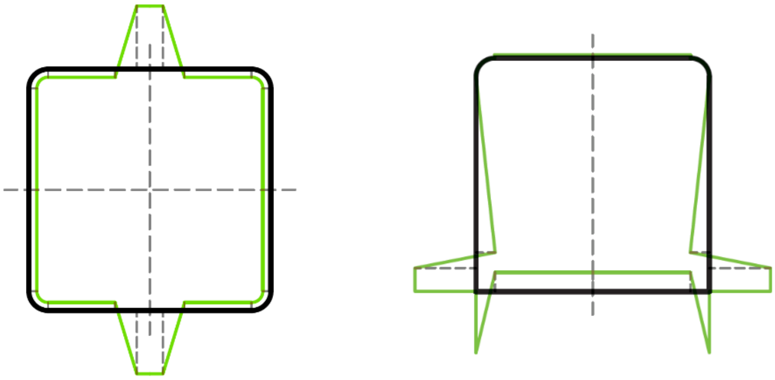

(a) Series SA section (b) Series SB section

Figure 2. Simplified longitudinal residual stress patterns

3. STOCKY COLUMN TESTS UNDER COMPRESSION

3.1. Test Programme

The section resistances of a total of eight stocky columns of S690 CFSHS are examined under compression, and the corresponding test programme is shown in Table 2. In order to avoid failure of overall buckling, these columns are designed to be short, i.e. their member lengths, L_m, are designed at 3h. Except for those stocky columns with Class 4 sections (Sections S2A and S2B), all stocky columns with Class 1 or 2 sections are expected to mobilize readily their full plastic resistances of the sections, and the measured maximum applied load, $N_{c,Et}$, should be larger than the design resistance of the section, $N_{c,Rd}$.

3.2. Test Results

Table 2 summarizes the key test results. It is shown that Sections S2A and S2B achieve only about 82% of their design resistances of the sections. For all the other sections, their measured section resistances are all larger than their design resistances. Figure 3 shows a direct comparison on the section resistance ratios, $\frac{N_{c,Et}}{N_{c,Rd}}$, against axial shortenings of various sections. Since Sections S3A and S3B have very small h/t ratios, they not only exceed their design resistances of the sections, but also exhibit high degree of ductility. Sections S2A and S2B fail to reach their design resistances of the sections because they are Class 4, and hence, a part of the cross-sectional area may be defined as non-effective that do not bear any compression. For Sections S1A, S1B, S4A and S4B, their measured section resistances just exceed their design section resistances with a limited degree of ductility. Although these four sections are Class 1 or 2 according to the current section classification rules of EN 1993-1-1 (BSI 2005), it is more reasonable to categorize them as Class 3 according to their low degree of ductility. Typical failure modes of these sections are shown in Figure 3, and it is found that there is no significant difference in the failure modes between Series SA and SB sections since local buckling occur at similar locations in these stocky columns.

Table 2. Test programme and results of stocky column tests

Series	Designation	Section classification	$N_{c,Rd}$	$N_{c,Et}$ (kN)	$\frac{N_{c,Et}}{N_{c,Rd}}$	Strength mobilization
SA	S1A-S	1	2459	2450	1.00	full
	S2A-S	4	3297	2745	0.83	--
	S3A-S	1	5502	5999	1.09	full
	S4A-S	1	6894	6914	1.00	full
SB	S1B-S	2	2459	2517	1.02	full
	S2B-S	4	3330	2719	0.82	--
	S3B-S	1	5604	5891	1.05	full
	S4B-S	2	7043	7108	1.01	full

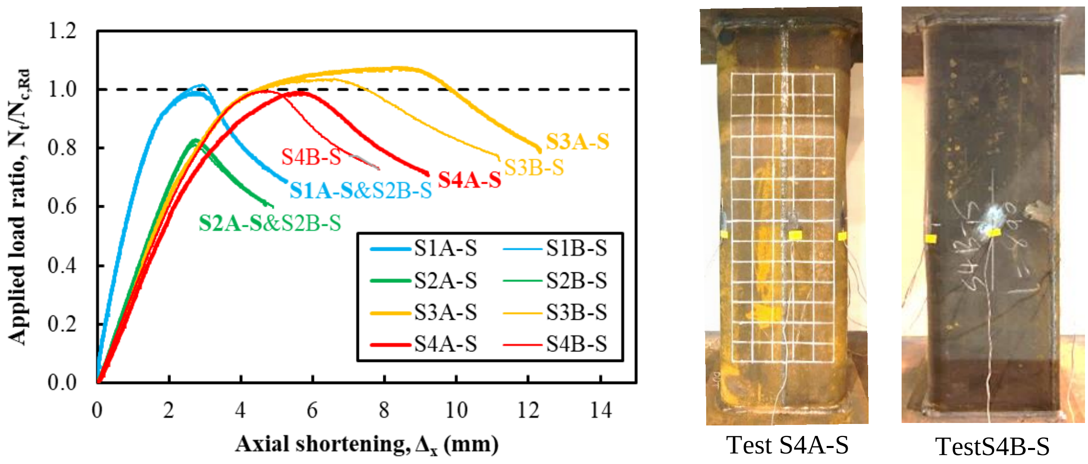

Figure 3. Applied load ratio-axial shortening curves and typical failure modes of stocky columns

4. SLENDER COLUMN TESTS UNDER COMPRESSION

4.1. Test Programme

In testing slender columns under compression, the most important structural parameter controlling failure modes of the columns is the slenderness ratio. In accordance with the design rules of EN 1993-1-1, the non-dimensional slenderness, $\bar{\lambda}$, plays a very important role in defining the member resistances of the slender columns. To evaluate the structural performance of these columns over a wide range of slenderness, two series of columns with different slenderness ratios are designed for each section in the current study, as shown in Figure 1. Thus, a total of 16 slender columns are tested under compression (see Table 3). It should be noted that the values of $\bar{\lambda}$ is designed to range from 0.3 to 0.9, and this allows an effective examination on certain reductions in the member resistances due to overall buckling.

Table 3. Test programme and results of slender column tests

Series	Designation	Section classification	$N_{c,Rd}$ (kN)	$\bar{\lambda}$	$N_{b,Rd}$ (kN)	$N_{b,Et}$ (kN)	$\frac{N_{b,Et}}{N_{b,Rd}}$	$\frac{N_{b,Et}}{N_{c,Rd}}$	Failure mode
SA	(1) S1A-P	1	2450	0.52	2039	2603	1.28	1.06	local
	(3) S2A-P	4	3295	0.46	2847	2981	1.05	0.91	overall
	(5) S3A-P	1	5524	0.40	4951	5448	1.10	0.99	overall
	(7) S4A-P	1	6933	0.38	6293	6867	1.09	0.99	overall
	(9) S1A-Q	1	2435	0.83	1565	2187	1.40	0.90	overall
	(11) S2A-Q	4	3392	0.56	2743	2913	1.06	0.86	overall
	(13) S3A-Q	1	5478	0.63	4220	4917	1.17	0.90	overall
	(15) S4A-Q	1	7010	0.51	5879	6698	1.14	0.96	overall
SB	(2) S1B-P	2	2485	0.55	2031	2477	1.22	1.00	overall
	(4) S2B-P	4	3341	0.48	2861	2724	0.95	0.82	overall
	(6) S3B-P	1	5598	0.42	4963	5556	1.12	0.99	overall
	(8) S4B-P	2	7102	0.39	6409	7149	1.12	1.01	overall
	(10) S1B-Q	2	2485	0.86	1547	2213	1.43	0.89	overall
	(12) S2B-Q	4	3438	0.58	2743	2852	1.04	0.83	overall
	(14) S3B-Q	1	5605	0.67	4181	5451	1.30	0.97	overall
	(16) S4B-Q	2	7110	0.53	5886	7027	1.19	0.99	overall

Note: $N_{b,Rd}$ is calculated with curve c (imperfection factor, α=0.49) according to the buckling design rules in EN 1993-1-1.

4.2. Test Results

Table 3 summarizes the test results of a total of 16 slender column tests under compression, where the measured maximum applied loads, $N_{b,Et}$, in each test is recorded. Besides, the design section resistance of the section, $N_{c,Rd}$, and the design member resistance of the column, $N_{b,Rd}$, are presented. It should be noted that $N_{b,Rd}$ in the current study is calculated based on the buckling curve c (imperfection factor, α=0.49) according to EN 1993-1-1 for member resistance design of slender columns of CFSHS against overall buckling. It should be noted that the ratios $\frac{N_{b,Et}}{N_{b,Rd}}$ of all slender columns with Classes 1 or 2 sections exceed 1.0. For those of Class 4 sections, there are parts of the cross-sectional area non-effective which have no contribution to their section resistances. For typical failure mode of these slender column tests, many of them fail in overall buckling. Figure 4 demonstrates typical relationships of the applied load against displacements of Test S3A-P. As depicted by Figure 4(a), there is a significant decrease in the applied load after reaching the maximum load. A similar trend is also evident in the applied load-horizontal displacement curve, as shown by Figure 4(b), where the horizontal displacement increases quickly after the maximum load is reached, and this indicates that an obvious overall buckling has occurred herein.

As above-mentioned, many of the slender column tests exceed their $N_{b,Rd}$ predicted by the buckling curve c, which means that it is too conservative to design these slender columns of CFSHS by simply adopting the current design rules of EN 1993-1-1. Figures 5 and 6 show differences in the member resistances between the slender columns of Series SA and SB sections. Obviously, the slender columns of Series SB sections have higher ratios $\chi\ (=\frac{N_{b,Et}}{N_{c,Rd}})$ than those of Series SA sections. Based on a direct comparison between the test results and the predictions provided by those buckling design curves (from curves a_0 to d) with different imperfection factors, α, it is reasonable to propose a design recommendation that both slender columns of Series SA and SB sections should be designed by using a buckling curve with a smaller value of imperfection factor, α.

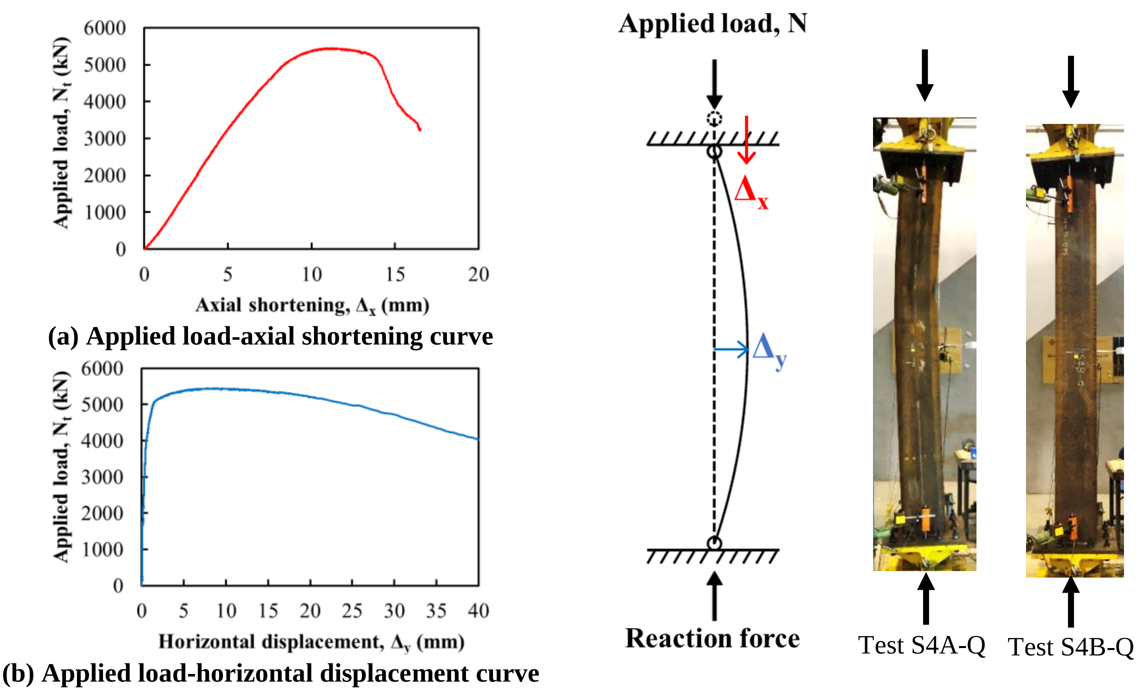

Figure 4. Applied load-displacement curves and typical failure modes of slender columns

5. CONCLUSIONS

In this paper, a total of eight cold-formed structural hollow sections (CFSHS) are examined, and an experimental investigation into the structural behaviour of 8 S690 CFSHS stocky columns under compression and 16 S690 CFSHS slender columns under compression are presented.

In general, all stocky columns with Class 1 and 2 sections are able to mobilize their full cross-section resistances, except Sections S2A and S2B which are Class 4 sections. Similarly, all slender columns with Class 1 and 2 sections are able to mobilize their member resistances, except Column S2B-P which is Class 4 section. Based on a direct comparison between the measured and the predicted resistances provided by those buckling design curves given in EN 1993-1-1, it is proposed to improve the design method such that a higher curve with a smaller imperfection factor should be used. Numerical models will be established after calibration against these test results, and both material and geometrical initial imperfections of these members with practical magnitudes will be incorporated to generate numerical resistances for development of the improved design method.

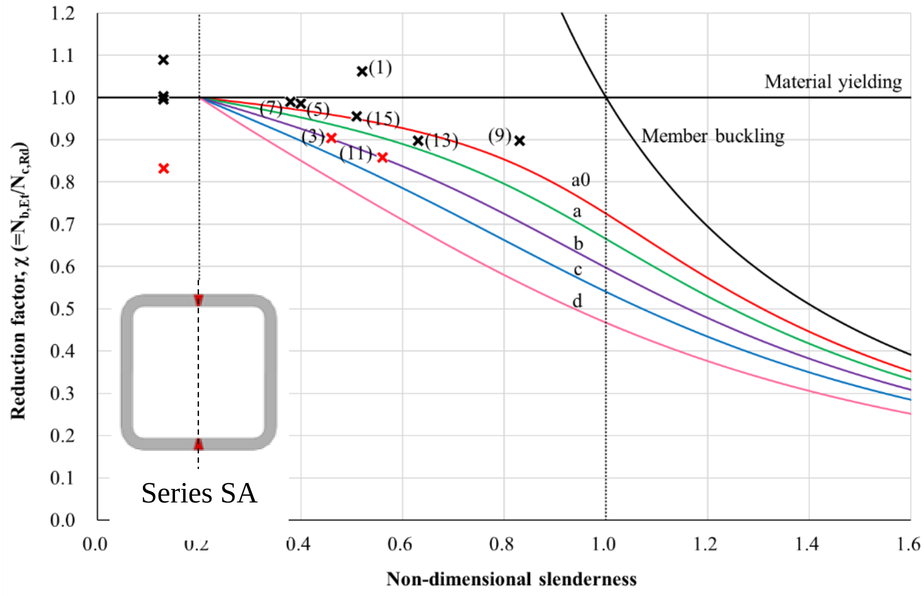

Figure 5. Design buckling curves and test data: EN 1993-1-1 and Series SA

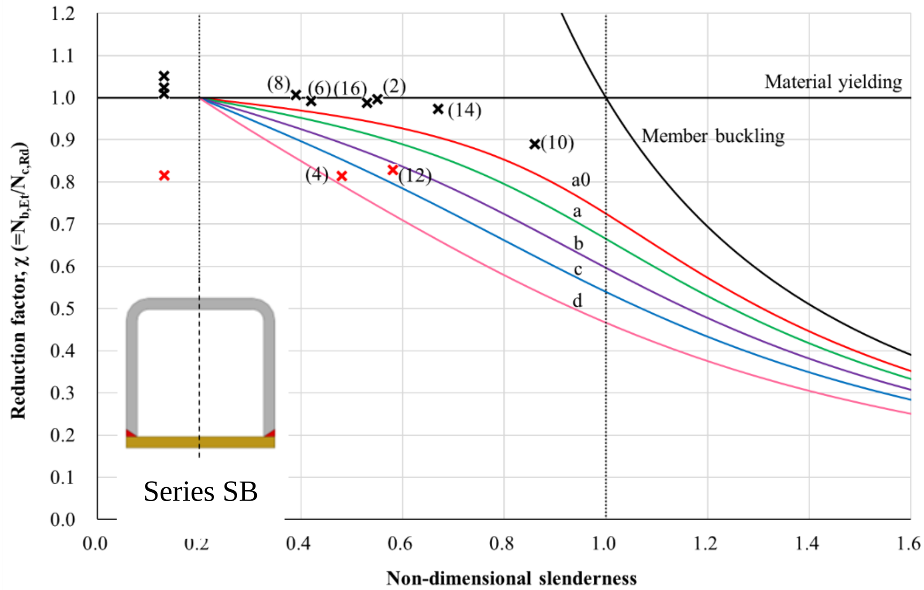

Figure 6. Design buckling curves and test data: EN 1993-1-1 and Series SB

ACKNOWLEDGEMENTS

The authors are grateful to the financial support provided by the Research Grant Council of the Government of Hong Kong SAR (Project Nos. PolyU 152687/16E and 152231/17E). The project leading to the publication of this paper is also partially funded by the Research Committee (Project No. RUQV) and the Chinese National Engineering Research Centre for Steel Construction (Hong Kong Branch) (Project No. 1-BBY3) of the Hong Kong Polytechnic University. The research studentship of the first author provided by the Hong Kong Polytechnic University is acknowledged. Special thanks go to the Nanjing Iron and Steel Company Ltd. in Nanjing, and to Dongguan Pristine Metal Works Ltd. in Dongguan. All structural tests on S690 CFSHS were carried out at the Structural Engineering Research Laboratory at the Hong Kong Polytechnic University, and supports from the technicians are gratefully acknowledged.

REFERENCES

BSI. (2005). EN 1993-1-1. Eurocode 3: Design of structures – Part 1-1: General rules and rules for buildings. British Standards Institution.

BSI. (2007). EN 1993-1-12. Eurocode 3: Design of structures – Part 1-12: Additional rules for the extension of EN 1993 up to steel grades S 700. British Standards Institution.

Goldak, J., Chakravarti, A., & Bibby, M. (1984). A new finite element model for welding heat sources. Metallurgical transactions B, 15(2), 299-305.

Hu, Y. F. (2019). Structural behaviour of high strength S690 steel cold-formed circular hollow sections (Doctoral dissertation, The Hong Kong Polytechnic University).

Li, T. J., Liu, S. W., Li, G. Q., Chan, S. L., & Wang, Y. B. (2016). Behaviour of Q690 high-strength steel columns: Part 2: Parametric study and design recommendations. Journal of Constructional Steel Research, 122, 379-394.

Liu, X., & Chung, K. F. (2018). Experimental and numerical investigation into temperature histories and residual stress distributions of high strength steel S690 welded H-sections. Engineering Structures, 165, 396-411.

Ma, T. Y., Hu, Y. F., Liu, X., Li, G. Q., & Chung, K. F. (2017). Experimental investigation into high strength Q690 steel welded H-sections under combined compression and bending. Journal of Constructional Steel Research, 138, 449-462.

Somodi, B., & Kövesdi, B. (2017). Flexural buckling resistance of cold-formed HSS hollow section members. Journal of Constructional Steel Research, 128, 179-192.

Wang, K. (2018). Study on structural behaviour of high strength steel s690 welded H-and I-sections (Doctoral dissertation, The Hong Kong Polytechnic University).

Wang, Y. B., Li, G. Q., Chen, S. W., & Sun, F. F. (2014). Experimental and numerical study on the behaviour of axially compressed high strength steel box-columns. Engineering Structures, 58, 79-91.

Yang, C., Yang, J., Su, M., & Li, Y. (2016). Residual stress in high-strength-steel welded circular tube. Proceedings of the Institution of Civil Engineers-Structures and Buildings, 170(9), 631-640.